Hemicellulose/PVA-based bioactive films for food packaging: Effect of the molecular weight of avocado pruning waste-derived hemicellulose on

International Journal of Biological Macromolecules 309 (2025) 142982

Contents lists available at ScienceDirect

International Journal of Biological Macromolecules

journal homepage: www.elsevier.com/locate/ijbiomac

Hemicellulose/PVA-based bioactive films for food packaging: Effect of the molecular weight of avocado pruning waste-derived hemicellulose on biocomposite properties

Andrea Lucena [a,b], Esther Rincón [a], Pamela Freire de Moura Pereira [c], Amparo Jiménez-Quero [c], Alejandro Rodríguez [a], Fernando Pérez-Rodríguez [b], Eduardo Espinosa [a,*]

[a] BioPrEn Group (RNM-940), Chemical Engineering Department, Instituto Químico para la Energía y el Medioambiente (IQUEMA), Faculty of Science, Universidad de Córdoba, 14014 Cordoba, Spain
[b] Department of Food Science and Technology, UIC Zoonosis y Enfermedades Emergentes ENZOEM, ceiA3, Universidad de Córdoba, 14014 Córdoba, Spain
[c] Division of Industrial Biotechnology, Department of Life Sciences, Chalmers University of Technology, 412 96 Gothenburg, Sweden

ARTICLE INFO

Keywords:
Food waste and loss
Tangential flow-diafiltration
Food active packaging films

ABSTRACT

The rising demand for sustainable packaging and urgent need for circular strategies in the agri-food sector motivate exploring biopolymer packaging from agri-food by-products. This study presents an efficient method for utilizing avocado pruning waste (APW) by extracting hemicelluloses for polyvinyl-alcohol (PVA)-based food packaging films. Autohydrolysis and tangential-flow diafiltration produced hemicellulose fractions with varying molecular weights: >50, 50–8, 8–1, and 1 kDa. High Mw-hemicelluloses exhibited high antioxidant power (>70 %) owing to their rich ferulic and trans-cinnamic acids, while low Mw-fractions demonstrated superior antimicrobial capacity, with a Minimum Inhibitory Concentration (MIC) and Minimum Bactericidal Concentration (MBC) against *L. monocytogenes* of 9 mg/mL and 14 mg/mL, respectively. Hemicellulose-enriched PVA-based films displayed heightened antioxidant capacity (>40 %) and excellent UV-light blocking efficiency (>80 %) with minimal transparency loss (80 %). Low Mw-range fractions decreased water solubility (8.4 % and 7.6 % for 5 % <1 kDa and 8–1 kDa films, respectively) enhancing water absorption properties (swelling degree of 766 % for 5 % <1 kDa and 992 % for 10 % 8–1 kDa films, respectively), whereas high Mw-range fractions strengthened mechanical properties and biodegradability (67 % and 59 % improvement, respectively). The differential effects of APW-derived hemicelluloses on PVA films underscore their potential as bio-based polymer source for the packaging industry, showing improved mechanical and bioactive properties.

1. Introduction

Lignocellulosic biomass, sourced from agriculture, forestry, and related industries, is rich in cellulose, hemicellulose, and lignin. Due to growing concerns about environmental sustainability, there is an increasing shift towards using lignocellulosic biomass as a substitute for petroleum-based products, aiming to maximize the value of biomass while minimizing environmental impact [1]. Avocado (*Persea americana*) cultivation has expanded in recent years, driven by the rising consumption of avocados and their derivatives, valued for their nutritional profile, especially their protein content and soluble vitamins [2]. Avocado crops undergo a biannual pruning to enhance productivity, which generates a significant amount of lignocellulosic biomass (780–1245 kg/ha annually, based on 100 trees per hectare, dry weight) [3]. Various studies have compared the antioxidant activity of different avocado components, highlighting that avocado pruning waste is a potential source of bioactive compounds and biopolymers like hemicelluloses [4].

Hemicellulose, which makes up 20–38 % of hardwood biomass, is a heteropolysaccharide with a branched structure, primarily composed of pentoses and hexoses, D-xylose, L-arabinose, D-mannose, and glucose as the main components. The type and proportion of these monomers, along with their bonds, determine the dominant type of hemicellulose in each plant species [5]. Autohydrolysis, which uses water at high

* Corresponding author.
E-mail addresses: b52luopa@uco.es (A. Lucena), esther.rincon@uco.es (E. Rincón), pamelaf@chalmers.se (P.F. de Moura Pereira), amparo@chalmers.se (A. Jiménez-Quero), a.rodriguez@uco.es (A. Rodríguez), b42perof@uco.es (F. Pérez-Rodríguez), eduardo.espinosa@uco.es (E. Espinosa).

https://doi.org/10.1016/j.ijbiomac.2025.142982
Received 24 June 2024; Received in revised form 21 March 2025; Accepted 7 April 2025
Available online 8 April 2025

pressure and temperature, is the most widely used and successful method for extracting and purifying valuable products like hemicelluloses from biomass. This process facilitates the solubilization of hemicelluloses, with oligosaccharides being the main reaction products, while the majority of the cellulose and lignin content remains largely unaltered [6]. Despite its selectivity, autohydrolysis often results in heterogeneous oligosaccharide populations, so the products are typically subjected to downstream processing techniques to yield purer and more homogeneous fractions. One such method is membrane processing, with ultrafiltration being recognized as a green downstream technique due to its low energy requirements and ease of use, making it relatively simple to scale up. Specifically, diafiltration, a post-treatment involving the dilution of the filtered fraction with water and repeated ultrafiltration cycles, is used to remove impurities to the desired level [7]. Thus, membrane processing stands as an eco-friendly tool in the pursuit of efficient and sustainable separation of different hemicellulose fractions.

Hemicelluloses have gained considerable attention in food packaging applications due to recent trends and regulations aimed at reducing plastic usage, driving the need for more sustainable and efficient alternatives. In packaging materials, hemicelluloses can serve a dual purpose: providing structural support and imparting bioactive properties that enhance the interaction between packaging and food, ultimately enhancing food shelf life. Their bioactive features are linked to factors such as molecular weight, structure, and monosaccharide composition [8]. However, hemicellulose-based materials have some disadvantages such as moisture sensibility, high hydrophilicity, poor mechanical properties which limit their practical application [9]. Different strategies are being followed to overcome these limitations including the chemical modification of hemicelluloses by esterification, etherification, grafting modification or cross-linking which result in hemicelluloses with enhanced film forming properties [5]. Despite the potential chemical modification to enhance their material properties, there are still some challenges such as the high costs, use of hazardous chemicals and generation of waste organic solvents [10]. In this context, hydrothermal extraction followed by diafiltration allows for the isolation of hemicelluloses with different molecular weights, facilitating the identification of the most suitable fraction for each application.

The objective of this study was to analyze how the physicochemical properties of hemicelluloses influence their bioactivity and reinforcing capacity in the production of biomaterials, identifying the fractions with the greatest potential for use in sustainable active food packaging. Avocado pruning waste was up-cycled using a green biorefinery approach, selectively extracting and characterizing their hemicelluloses for incorporation into Polyvinyl Alcohol (PVA) active food packaging films, studying the influence of hemicellulose molecular weight and chemical composition.

2. Materials and methods

2.1. Materials

Avocado pruning waste (APW) was provided by a local farmer from an avocado crop in Salobreña (Spain) in mid-April 2023. APW was dried and stored at room temperature in a dark room until use. Once dried, it was ground in a Retsch SM 2000 mill to obtain a particle size of 0.25–0.40 mm. The raw material was characterized for its chemical composition following the Technical Association of the Pulp and Paper Industry (TAPPI) standard methods including extractives (T-204), holocellulose (T-9wd75), lignin (T-T-222), α-cellulose (Tappi T-429) and ash (T-211. These analyses were performed in triplicate [11]. Details on these procedures are included in Supplementary material.

2.2. Water autohydrolysis and tangential-flow diafiltration

APW-derived hemicelluloses were obtained by means of an autohydrolysis and subsequent tangential-flow diafiltration to sort them into different molecular weight (Mw) groups (Scheme S1). The water autohydrolysis process was carried out in a 15 L batch reactor employing an outer jacket heater and a rotating shaft for agitation. 1 kg (over dry matter) of APW was subjected to the following autohydrolysis conditions (Log R_0 3.5): 10 min, 185 °C and a liquid:solid ratio of 5. Two primary fractions were yielded from this process: the remaining solid residue of APW (Aut-R) and the liquor containing the dissolved APW-derived hemicelluloses (Aut-L). Aut-R was characterized following the TAPPI standards as stated for the APW.

The fraction Aut-L was submitted to a tangential-flow diafiltration on a Ultrafiltrator Pall Membralox Benchtop Crossflow Pilot Unit and 10 mm diameter INSIDE Céram™ membranes (TAMIS Industries Les Laurons, France). The diafiltration process was performed successively under different molar mass-cut off (MMCO) membranes (50, 8 and 1 kDa) to separate the hemicelluloses by Mw ranges. Four different hemicellulose fractions were obtained with different Mw ranges: >50 kDa, 50–8 kDa, 8–1 kDa and <1 kDa. The four isolated fractions and Aut-L were freeze-dried before characterization and subsequent application.

2.3. Characterization of avocado pruning waste-derived fractions

2.3.1. Chemical characterization of liquor and hemicellulose fractions

Both Aut-L and the four fractions from the tangential-flow diafiltration were evaluated for pH, conductivity, and total soluble solids (TSS). pH was measured with a Crison GLP 21 pHmeter (Crison pH Instruments, Barcelona, Spain). Electric conductivity was determined with a Crison GLP 31 EC meter (Crison Instruments, Barcelona, Spain). TSS were gravimetrically measured by drying 2 mL of the sample at 105 °C for 24 h.

Chemical characterization of both Aut-L and the four fractions resulting from the tangential-flow diafiltration consisted of the determination of molar mass distribution by size-exclusion chromatography, protein content by dye-binding assay, starch content, monosaccharide composition by high-performance anion-exchange chromatography coupled to pulsed amperometric detection (HPAEC-PAD), and phenolic acids by high-performance liquid chromatography (HPLC). Further details on these procedures are included in the Supplementary material.

2.3.2. Antioxidant activity of avocado pruning waste-derived fractions

To obtain an accurate estimation of the antioxidant activity of Aut-L and different Mw-range hemicelluloses, it was measured by two different assays: antioxidant power by ABTS method (AOP) and radical scavenging activity by DPPH method (RSA). For both methods, mmol of Trolox Equivalent (TE) per dry weight (DW) were obtained as well. Antioxidant power by ABTS method (AOP) and radical scavenging activity by DPPH method (RSA) were performed as described by Espinosa et al. with some modifications [12]. For ABTS method, a radical 7 mM ABTS solution in 2.44 mM $K_2O_8S_2$ was prepared and incubated in darkness for 16 h before use. Then, an ethanol:water 50 vol% solution was used to dissolve the ABTS radical solution until an absorbance of 0.7 ± 0.02 at 734 nm. Then, 20 μL of the different hemicellulose fractions were mixed with 180 μL of ABTS solution in a microplate. These mixtures were incubated during 5 min at 30 °C in darkness and their absorbance at 734 nm was recorded in a Microplate Reader EZ Read 400, Biochrom (Cambridge, UK). For DPPH method, a radical 0.2 mM DPPH solution in methanol was prepared. Then, the DPPH solution was diluted until an absorbance of 2 at 517 nm was obtained. Then, 10 μL of sample was mixed with 310 μL DPPH solution in a microplate as well. In this case, the mixtures were incubated during 30 min at room temperature in darkness and their absorbance at 517 nm was recorded as stated for the ABTS assay. Trolox was used to build a calibration curve and express the results as μmol of Trolox Equivalent (TE) per DW. All the measurements were performed in triplicate and the results were expressed as the arithmetic mean with its standard deviation.

2.3.3. Antimicrobial capacity of avocado pruning waste-derived fractions

The antimicrobial potential of hemicelluloses was assessed against different pathogens to determine the minimum inhibitory concentration (MIC) and minimum bacterial concentration (MBC). MIC value represents the lowest hemicellulose concentration at which pathogens are not able to grow, while the MBC stands for the lowest hemicellulose concentration that result in pathogen inactivation. The following foodborne pathogens were used during this study: *Escherichia coli* CETC 4076; *Listeria monocytogenes* CETC 4032; *Listeria monocytogenes* 3254 facilitated by the Collection of Microorganisms of the Junta de Andalucía (Andalusia, Spain); *Salmonella enterica* CETC 704; and two different *Staphylococcus aureus* (*S. aureus* 103 and *S. aureus* 33) isolated from artisanal goat industry and cheese [13]. All these pathogens were provided from Spanish Collection of Type Culture (CECT, Valencia, Spain) and all the culture media used were provided from Condalab (Madrid, Spain).

The MIC was determined using the method described by Sánchez-Gutiérrez et al. with some modifications [14]. Briefly, samples concentrations in the range of 0.5–20 mg/mL were prepared for the different hemicellulose fractions and autoclaved at 121 °C during 15 min. In a 96-well microplate, samples were inoculated with 10^5 CFU/mL suspension in Muller Hilton Broth (MHB) for each strain. All conditions were tested in triplicate. Negative controls were added in the microplate, one for MHB medium and another for each concentration of hemicelluloses. In addition, positive controls were also prepared in MHB for all bacteria and included in the microplates. Microplates were incubated for 24 h at 37 °C. Then, 50 μL of 0.01 *w/v*% resazurin was added and incubated for 2 h at 37 °C. After this time, counts in wells showing no color change were enumerated by spread plate method on Plate Count Agar (PCA) for confirming no growth or population reductions. Those samples with similar or not significant increase in the value of CFU (10^5 CFU/mL) were used to derive MIC values while wells presenting no colonies in PCA were used to determine MBC values.

2.4. PVA-based films fortified with avocado hemicelluloses

PVA-based films were produced using the solvent casting technique with a grammage of 35 g/m^2. First, a 2.8 *w/v*% PVA aqueous stock solution was prepared through magnetic stirring over 3 h at 80 °C. To prepare films with increasing hemicellulose contents (ranging from 5 wt % to 20 wt% on PVA's DW), PVA solution was blended with varying hemicellulose quantities from the different fractions. Distilled water was added to the blend to reach a final volume of 100 mL, resulting in a film-forming solution with a 0.2 wt% concentration. The solution was homogenized, at room temperature, with magnetic stirring until complete solubilization and mixing. Subsequently, the film-forming solution was poured into 12 × 12 cm Petri dishes and left until complete evaporation. All produced films were subjected to a 3-day conditioning phase at 25 °C and 50 % relative humidity (RH) prior to characterization.

2.5. Characterization of the films

2.5.1. Thickness

Films thickness (mm) was assessed with a Digital Micrometer IP65 0-1″ Digimatic Mitutoyo (Neuss, Germany) with a sensitivity of 0.001 mm. Five random measurements for each film were performed.

2.5.2. Antioxidant activity

The antioxidant activity was determined by means of the DPPH assay and the ABTS method as aforementioned explained with some modifications reported in Supplementary material.

2.5.3. Antimicrobial capacity

The antimicrobial activity of film samples was tested using the agar diffusion method, according to the protocol described by Rincón et al. with modifications [15]. Briefly, *Escherichia coli* CETC 4076, *Listeria monocytogenes* CETC 4032, *Salmonella enterica* CETC 704 and a *Staphylococcus aureus* 103 [13]. Inoculum was prepared as previously described in Section 2.3.3. Fresh cultures of microorganisms were inoculated on the surface of MHA medium with a concentration of 10^8 CFU/mL once adjusted to the 0.5 McFarland turbidity Standard. Film cuts with a 2 × 2 cm size, previously sterilized with UV-light during 30 min, were placed on the surface of the plates in triplicates. Two negative controls were performed, one for MHA medium and another for PVA film control. In addition, positive controls were prepared for all bacteria. Plates were incubated for 24 h at 37 °C. After the incubation, the antimicrobial activity of the test was evaluated determining the antibacterial inhibition halo.

2.5.4. Optical properties: transparency and UV-barrier

Optical properties in terms of transparency and UV-light barrier were determined using a 7315 Spectrophotometer Jenway (Stone, Staffordshire, UK) Light transmittance of the film rectangular pieces (1 × 3 cm) at 660 (%T_{660}) and 280 nm (%T_{280}) were measured in triplicate. Transparency and UV-barrier properties were calculated according to the following formulas:

$$\text{Transparency}\ (\%) = \frac{log\%T_{660}}{thickness(mm)}$$

$$UV-barrier\ (\%) = 100 - \left(\frac{\%T_{280}}{\%T_{660}} \cdot 100\right)$$

2.5.5. Mechanical properties

The Young Modulus (YM), Tensile Strength (TS) and strain-stress curves were determined in accordance with ASTM D882 standard method [16]. A LF Plus Lloyd Instrument (AMETEK Measurement & Calibration Technologies Division, Largo, FL, USA) was used as testometric tensile tester to assess the mechanical properties of film samples. Analyses were performed in film specimens of 1.5 cm × 10 cm. The initial separation between grips was 70 mm and the crosshead speed and load cell were fixed at 10 mm/min and 1kN, respectively. Results were expressed as an average of six samples for each type of film.

2.5.6. Solubility in water and swelling degree

Swelling degree (SD, %) was determined as the percentage of moisture gained after leaving dried film pieces of 1 cm^2 in water during 24 h and solubility in water (SW, %) was assessed as the percentage of film DW which was solubilized. In order to obtain these values, 50 mL of distilled water was used to immerse the dry film samples under magnetic stirring during 24 h at room temperature. The water was removed, and the films were weighed to know the percentage of moisture gained (SD). Then, the film pieces were oven-dried at 105 °C for 24 h and weighed again to find out the percentage of solubilized DW (SW).

2.5.7. Water vapor permeability

Water vapor permeability (WVP) was determined as reported in previous investigations [13,17], evaluated as described in ASTM E96/E96-10 standard method [18] using TQC Sheen Permeability Cups (Industrial Physics, Boston, MA, USA) of an anodized aluminum with 10 cm^2 surface area and a desiccant material, $CaCl_2$ was placed inside. The permeability cups were placed in climatic chamber ICHeco (Memmert, Büchenbach, Germany) at 25 °C and with 50 % RH. Mass gains were measured at different periods of time over a period of 24 h. The obtained data were used in the following formulas to quantify the water vapor transmission rate (WVTR) and the WVP:

$$\text{WVTR} = \frac{G}{t \cdot A}$$

where G is the weight gain (g), t the time (h) during which G occurred, and A is the film area (m^2).

$$\mathrm{WVP} = \frac{WVTR}{S(R_1 - R_{2)}}$$

where S is the saturated vapor pressure (Pa), and R_1 and R_2 are the relative humidities at the source and at the vapor sink, respectively, expressed as a fraction.

All the properties were determined in triplicate and the results were expressed as the arithmetic mean with its standard deviation.

2.5.8. Degradation of films during soil burial

The biodegradability of the films was evaluated by a degradation study during burial in soil was conducted following the methodology described by Morcillo-Martín et al. [19]. In brief, square film pieces of 4 cm^2 were buried in commercial compost at a depth of approximately 10 cm, under controlled conditions of 25 °C and 50 % relative humidity (RH) for 50 days. After this period, the films were recovered, washed with distilled water, and dried in an oven at 60 °C until constant weight. Biodegradability of the materials was expressed as weight loss (WL) of the films after the burial period and calculated using the following formula:

$$WL\ (\%) = \frac{Wi - Wf}{Wi} \cdot 100$$

where Wi is the initial weight of the film before burial, and Wf is the final weight of the film after drying.

2.6. Statistics

All data have been represented as the average ± standard deviation. Data have been analyzed by analysis of variance (ANOVA) followed by the Duncan test. In the case of the APW and Aut-R chemical characterization data (contained in Table 1), the differences between results have been analyzed using Student's *t*-test for independent samples. Statistical analysis were performed with SPSS software and are indicated as different letters that show significant differences ($p \leq 0.05$).

3. Results and discussion

3.1. Characteristics of avocado pruning waste-derived fractions

The chemical composition (and consequently, the valorization potential) of avocado-by products, varies significantly among the different by-products derived from avocado production. Table 1 presents the chemical composition of the APW. The carbohydrate content, pool of cellulose and hemicelluloses, was similar to that found in the peel and seed (43 %) [20]. On the contrary, peel and seed presented a higher extractable content (>35 %) than that of pruning, primarily due to the presence of phenolic compounds. Additionally, the lignin content in peel and seed (1.8–4.4 %) was significantly lower than in APW, which is attributed to the woody and lignocellulosic nature of the latter.

In the context of valorization through biorefinery processes, developing multi-product approaches that leverage existing industrial facilities becomes essential. Consequently, the valorization of APW assumes greater significance compared to other fractions. In the initial stage of the biorefinery process, extracting hemicelluloses is a logical precursor to the extraction of cellulosic fibers and the removal of lignin [21]. The hemicellulose content in APW is comparable to that found in other agricultural residues such as bay tree pruning, vine shoots, or olive tree pruning used for the extraction of this fraction with high yields, suggesting the suitability of APW for this purpose [22,23].

Table 1
Chemical composition (%) of avocado pruning waste (APW) and autohydrolysis remaining solid residue (Aut-R).

	APW	Aut-R
Hot-water extractable	17.45 ± 1.61[a]	7.19 ± 0.48[b]
Ethanol extractives	19.77 ± 1.29[a]	19.52 ± 1.45[a]
Hemicelluloses	21.42 ± 1.29[a]	8.77 ± 2.23[b]
Lignin	21.09 ± 1.90[b]	37.81 ± 2.09[a]
α-Cellulose	27.91 ± 2.71[b]	44.20 ± 0.65[a]
Ash	5.96 ± 0.12[a]	3.67 ± 0.56[b]

Different superscript letters show significant differences ($p \leq 0.05$).

The severity of the autohydrolysis treatment has a significant effect on the efficiency of polysaccharide extraction and its integrity. In previous work, Rincón et al., demonstrated that the highest polysaccharide extraction yields are in the range Log R_0 3.2–3.7, with intermediate values showing higher polysaccharide integrity [20]. To favor the extraction of polysaccharides from APW with the highest possible preservation, a Log R_0 of 3.5 was selected. The efficiency of the hemicellulose extraction process was assessed using the mass balance from the autohydrolysis process (Fig. 1), taking into account the stage yields and the chemical composition of APW and Aut-R (Table 1).

At this stage, the extraction yield of hemicellulose reached 71.85 % of the total hemicellulose in APW, resulting in an extraction of 15.39 g per 100 g of APW, from a total of 21.42 of hemicellulose contained in APW. Additionally, an analysis of the hemicellulose-enriched liquor (Aut-L) following sequential ultrafiltration demonstrated the efficiency of the extraction process, while the process severity effectively preserved the structural integrity of the hemicelluloses. Notably, >71 % of the extracted hemicelluloses exhibited higher Molecular weight (Mw) with values of 37.32 % in the >50 kDa fraction and 33.80 % in the 50–8 kDa fraction, corresponding to Mw values of 20.37 and 2.50 kDa, respectively. In contrast, the remaining 29 % of the hemicelluloses were distributed across the lower Mw fractions, with 13.62 % in the 8–1 kDa fraction and 15.62 % in the <1 kDa fraction exhibiting Mw values of 1.18 and 1.20 kDa, respectively. The extraction process used was suitable for obtaining high yields with preserved structures, which corroborates the suitability of the downstream process: efficiency in the extraction and separation of hemicelluloses [24].

Parameters such as pH, conductivity, and total soluble solids (TSS) were evaluated for all the liquid fractions (Table 2). A general increase in acidity, characteristic of autohydrolysis processes, was noted following the release of acetyl groups, leading to the formation of acetic acid, and phenolic groups in the medium [25,26]. Notably, Aut-L exhibited the highest conductivity and TSS values, indicating the high concentration of hemicelluloses. After the various stages of ultrafiltration, the highest conductivity values were observed for the >50 kDa and 50–8 kDa fractions, 2.78 and 2.32 mS/cm, respectively, with corresponding TSS values of 15.90 and 14.40 mg/mL. These values were consistent with the biomass balance and indicate a significant higher concentration of hemicelluloses in these fractions compared to the lower Mw fractions which showed conductivity values of 1.87 mS/cm and TSS values of 5.80 mg/mL and 1.86 mS/cm and 6.50 mg/mL for 8–1 kDa and < 1 kDa fraction, respectively.

The molar mass distribution of the various hemicellulose fractions was verified by SEC analyses as shown in Fig. 2A. The Aut-L fraction exhibited a bimodal distribution, with low and high molar mass between 10^3 and 10^5 Da, indicating the presence of two distinct macromolecular populations. In contrast, all treated samples achieved monodisperse populations, with polydispersity decreasing as the processing molar mass cut-off (MMCO) membranes were utilized during tangential-flow diafiltration. This suggests that tangential-flow diafiltration using MMCO membranes >50 kDa may effectively remove fractions between 10^4 and 10^5 Da, potentially including soluble proteins and starch. Notably, no differences were observed between MMCO with 8–1 kDa and < 1 kDa, with weight-average molar mass very similar corresponding to 1.18 kDa and 1.20 kDa, respectively (Table 2). Monosaccharide composition distribution of different fractions of APW is shown in Fig. 2B. In the Aut-L fraction, xylose (43.07 %) significantly exceeded glucose (13.58 %) content, followed by mannose (29.24 %), glucose (13.58 %), galactose (8.54 %), and arabinose (3.64 %) (Table 3),

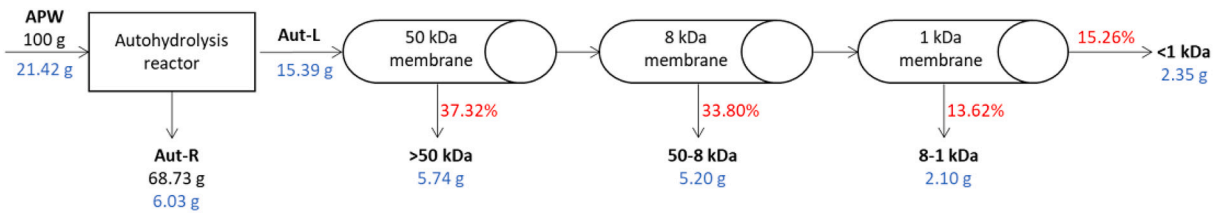

Fig. 1. Mass balance of hemicellulose extraction process (*hemicellulose balance by weight is shown in blue letters, while the total weight balance in black lettering*).

Table 2
Values of pH, conductivity, total soluble solids (TSS), chemical composition and molar mass distribution data of APW-hemicellulose derived fractions obtained after autohydrolysis and tangential-flow diafiltration.

		Aut-L	>50 kDa	50–8 kDa	8–1 kDa	<1 kDa
pH		4.32 ± 0.01^{e}	4.34 ± 0.00^{d}	4.38 ± 0.01^{c}	4.56 ± 0.01^{b}	4.59 ± 0.01^{a}
Conductivity (mS/cm)		6.75 ± 0.02^{a}	2.78 ± 0.02^{b}	2.32 ± 0.02^{c}	1.87 ± 0.02^{d}	1.86 ± 0.01^{d}
TSS (mg/mL)		41.3 ± 0.80^{a}	15.90 ± 1.20^{b}	14.40 ± 0.80^{b}	5.80 ± 1.60^{c}	6.50 ± 1.00^{c}
Soluble protein (mg·g^{-1} DW)*		3.81 ± 0.17^{b}	6.54 ± 0.99^{a}	4.37 ± 0.62^{b}	4.34 ± 0.25^{b}	1.93 ± 0.40^{c}
mg·g^{-1} DW**	Carbohydrate content	248.60 ± 32.69^{a,b}	317.37 ± 42.55^{a}	361.69 ± 61.77^{a}	241.03 ± 65.34^{a,b}	196.80 ± 4.64^{b}
	Starch content***	36.20 ± 1.20^{a}	39.20 ± 4.30^{a}	42.80 ± 11.10^{a}	24.80 ± 2.80^{b}	19.10 ± 0.10^{b}
	β-Glucan†	99.64 ± 0.10^{a}	99.79 ± 0.04^{a}	98.28 ± 7.13^{a}	75.28 ± 0.30^{b}	77.76 ± 0.02^{b}
	Phenolic acids‡	4.19 ± 0.11^{b}	3.98 ± 0.11^{b}	3.25 ± 0.31^{b}	5.84 ± 0.26^{a}	5.69 ± 0.12^{a}
kDa	Mn	2.07	1.53	1.78	1.04	1.04
	Mw	11.56	20.37	2.50	1.18	1.20

Different superscript letters show significant differences ($p \leq 0.05$).
* Soluble protein content determined by Bradford method and expressed in mg albumin eq.g of dry weigh^{-1}.
** DW: dry weight.
*** Determined by enzymatic hydrolysis.
† Difference between glucose content from methanolysis and α-glucans from starch analysis.
‡ Determined by HPLC.

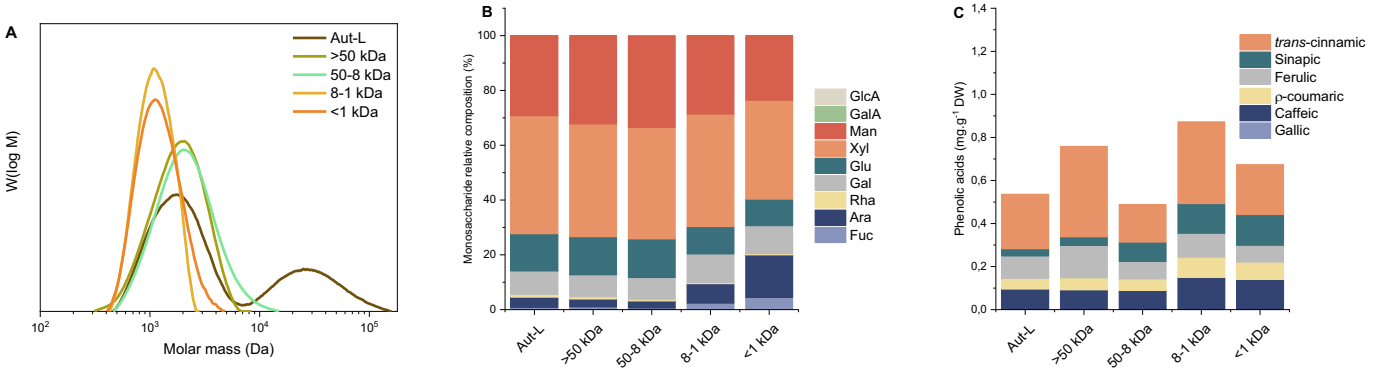

Fig. 2. Molar mass distribution (A), monosaccharide profiling (B) and phenolic acids profile of the different fractions from APW (C).

suggesting the major presence of xyloglucan-type hemicelluloses. According to Ankona et al. avocado trees have combined properties of hardwood and softwood [27]. This might explain the presence of a significant portion of mannose as possibly derivative mannans, such as galactoglucomannans, commonly found in softwoods [28]. The used MMCO affected hemicelluloses composition. Thus, the part of xyloglucans presented the highest molecular mass, supported by the slight decrease of xylose content from the Aut-L to the first fraction obtained at MMCO >50 kDa (41.17 %). This trend was also accompanied by the disappearance of high Mw population peak in SEC results (Fig. 2A). Increasing the cut-off to 8–1 kDa leads to a significant decrease in glucose (10.01 %) and mannose (28.63 %), accompanied by increase of arabinose (7.12 %) and fucose (2.35 %) concentrations in relation to the other monosaccharides, which are concentrated due to the lower molecular weight.

The presence of soluble proteins and starch was also evaluated to verify the fractionated hemicelluloses purity (Table 2). Both compounds decreased as the diafiltration process progressed, indicating the retention of protein and starch molecules in higher cut-off membranes, yielding extracts with higher purity in hemicelluloses.

Phenolic acid contents in APW-derived fractions are shown in Fig. 2C. Despite biomass recalcitrance, some phenolic acids were significantly present in lower Mw fractions (8–1 kDa and <1 kDa) such as caffeic acid (0.15 ± 0.01 and 0.14 ± 0.02 mg·g^{-1} DW, respectively), *p*-coumaric (0.09 ± 0.00 and 0.08 ± 0.01 mg·g^{-1} DW, respectively) and sinapic acid (0.14 ± 0.00 mg·g^{-1} DW for both of them). In contrast, *trans*-cinnamic acid was present in high amounts (0.23–0.42 %) (Table 4), indicating that the autohydrolysis was able to recover a

Table 3
Carbohydrate composition (%) of the different APW-derived hemicellulose fractions.

	Fucose	Arabinose	Rhamnose	Galactose	Glucose	Xylose	Mannose
Aut-L	0.87 ± 0.08^{c}	3.64 ± 0.25^{b}	1.05 ± 0.18^{a}	8.54 ± 0.77^{a}	13.58 ± 1.12^{a}	43.07 ± 0.61^{a}	29.24 ± 0.45^{a}
>50 kDa	1.01 ± 0.12^{c}	2.83 ± 0.45^{b}	0.84 ± 0.09^{a,b}	8.03 ± 0.90^{a}	13.89 ± 0.39^{a}	41.17 ± 3.00^{a}	32.22 ± 4.52^{a}
50–8 kDa	0.62 ± 0.10^{c}	2.55 ± 0.41^{b}	0.62 ± 0.38^{a,b,c}	7.91 ± 0.72^{a}	14.11 ± 1.82^{a}	40.68 ± 0.79^{a}	33.52 ± 3.49^{a}
8–1 kDa	2.35 ± 0.47^{b}	7.12 ± 0.24^{b}	0.52 ± 0.05^{b,c}	10.31 ± 0.22^{a}	10.01 ± 0.25^{b}	41.05 ± 0.85^{a}	28.63 ± 1.70^{a}
<1 kDa	4.54 ± 0.12^{a}	15.44 ± 0.41^{a}	0.47 ± 0.03^{c}	10.18 ± 0.22^{a}	9.68 ± 0.10^{b}	36.09 ± 0.67^{b}	23.60 ± 0.61^{b}

Different superscript letters show significant differences ($p \leq 0.05$).

significant amount of this compound. Overall, the presence of phenolic acids in APW fractions also suggested that autohydrolysis solubilized APW-hemicelluloses while preserving its covalently bound phenolic acid structure [16,29,30].

The results of antioxidant power (AOP, determined by the ABTS method) and radical scavenging activity (RSA, determined by the DPPH method) these tests are shown (Fig. 3). The antioxidant capacity was attributed to both phenolic content and the reductive carbohydrate structure present in hemicelluloses [31]. In a broader context, Aut-L exhibited a remarkable antioxidant potential with values of 55.15 % and 54.10 % for AOP and RSA, respectively. All Mw-range fractions demonstrated notable antioxidant activity, with the >50 kDa fraction displaying the highest efficacy. Guo et al., 2021 emphasized that the differences in the antioxidant activity of various xylan fractions can be attributed to non-carbohydrate components, particularly phenolic compounds like phenolic acids, and proteins [32]. This correlation is supported by the data observed in <50 kDa fraction, exhibiting significantly the highest soluble protein content (6.54 mg·g^{-1} DW) in Table 2. It is noteworthy that the AOP values slightly surpassed those of RSA, with the disparities attributed to the distinct reduction mechanisms exhibited by the radicals involved [17]. These results underscore the efficacy of autohydrolysis in recovering a substantial quantity of hemicelluloses while preserving their inherent structure, thereby enhancing their antioxidant activity and suggesting the suitability of APW-hemicelluloses for food and pharmaceutical applications [33].

The results of the antimicrobial test, which assessed both the bacteriostatic and bactericide effect of APW-derived hemicellulose fractions are summarized in Table 5. The MIC and MBC results of the Aut-L fraction revealed the bioactivity of APW-hemicelluloses. Remarkably, the <1 kDa fraction exhibited antimicrobial activity comparable to that of Aut-L, suggesting its crucial role in conferring bioactivity to the latter. Specifically, the highest bactericide activity was found for <1 kDa against L. *monocytogenes* 3254. The maximum bacteriostatic activity corresponded to Aut-L, >50 kDa and <1 kDa with a MIC 9 mg/mL against *L. monocytogenes* (3254) as well. The antimicrobial properties of hemicelluloses are influenced by multiple factors, including their phenolic profile, molecular weight, and sugar composition [34]. Diverse mechanisms have been proposed, ranging from the destruction of bacterial membrane, inhibition of biofilm, impediments to the bacterial colonization, inhibition of quorum sensing, binding of metabolites and inhibition of efflux pump of polysaccharides which complicates the survival of foodborne pathogens [35]. Additionally, certain phenolic compounds, like caffeic acid, have demonstrated potent antimicrobial activity attributed to the presence of hydroxyl groups on its phenolic ring, rendering it effective against foodborne pathogens [36]. Sinapic acid, for instance, has exhibited substantial antibacterial properties against phytopathogens, such as *Xylella fastidiosa*, with an MIC value of 1 mg/mL [37]. Therefore, the elevated content of such phenolic compounds in the <1 kDa fraction (0.14 mg·g^{-1} DW for caffeic acid and sinapic acid, Table 4) could plausibly account for its pronounced bioactivity.

Table 4
Phenolic acids composition (mg·g^{-1} DW) of the different APW-derived hemicellulose fractions.

	Caffeic acid	*p*-Coumaric acid	Ferulic acid	Sinapic acid	Trans-cinnamic acid
Aut-L	0.10 ± 0.00^{b}	0.05 ± 0.00^{b}	0.10 ± 0.01^{b,c}	0.03 ± 0.00^{b}	0.25 ± 0.01^{a,b}
>50 kDa	0.09 ± 0.00^{b}	0.06 ± 0.01^{b}	0.15 ± 0.01^{a}	0.04 ± 0.00^{b}	0.42 ± 0.01^{a}
50–8 kDa	0.09 ± 0.01^{b}	0.05 ± 0.01^{b}	0.08 ± 0.01^{c}	0.09 ± 0.00^{b}	0.17 ± 0.02^{b}
8–1 kDa	0.15 ± 0.01^{a}	0.09 ± 0.00^{a,b}	0.11 ± 0.02^{b}	0.14 ± 0.00^{a}	0.38 ± 0.02^{a}
<1 kDa	0.14 ± 0.02^{a}	0.08 ± 0.01^{a}	0.08 ± 0.01^{c}	0.14 ± 0.00^{a}	0.23 ± 0.01^{a,b}

Different superscript letters show significant differences ($p \leq 0.05$).

3.2. Effects of APW-hemicelluloses in PVA films and their characteristics

Based on the characterization of APW-hemicelluloses, APW-by products demonstrated promising properties as active ingredient for packaging materials, enhancing the performance of existing solutions. The subsequent step of this study aimed to assess the contribution of different Mw-ranges APW-hemicelluloses to the bioactive properties in PVA films. For this purpose, each Mw-range fraction was studied at increasing proportions in the films (5, 10, 15, and 20 wt%).

3.2.1. Active properties of APW-enriched PVA-based films

The antioxidant power (AOP) of PVA films containing APW-hemicelluloses analyzed by ABTS assay is shown in Fig. 4A–B. The results demonstrated significant antioxidant activity compared to the control PVA films. All molecular weight range fractions of hemicelluloses exhibited high antioxidant capacity, largely due to their polysaccharide content such as galactoglucomannans and xyloglucans and their associated phenolic content [38]. Notably, this antioxidant power significantly increased when the proportion of hemicelluloses in the matrix was higher (15–20 wt%) regardless of the Mw. Interestingly, the >50 kDa fraction did not show the highest radical scavenging capacity, which may be attributed to the structural and spatial arrangement of the hemicelluloses within the PVA matrix. Previous studies have reported that high molecular weight components, such as lignin, can promote aggregation, reducing the mobility and obscuring functional groups that interact with the environment [39]. The enhanced antioxidant activity of the hemicellulose-enriched PVA films suggests that this APW-hemicellulose fraction could be a suitable candidate as an active ingredient for food packaging. However, as expected, the APW hemicellulose-enriched PVA films had not antimicrobial activity (Figs. S1–S4). This was attributed to the fact that the concentration of hemicelluloses used was below the MIC previously determined.

3.2.2. Optical properties of the bioactive APW-hemicellulose films

The effect of different APW-hemicellulose fractions on transparency (%) and UV-light blocking ability (%) is shown in Fig. 4C–D. As the hemicellulose content increased, a decline in transparency was observed resulting in slight opaqueness in the films. However, films including low Mw-range fractions (8–1 kDa and <1 kDa) or those with 5 wt% hemicelluloses showed similar transparency values to the control PVA films. This suggests that lower Mw-range fractions, characterized by smaller molecular diameters and reduced soluble protein and starch content,

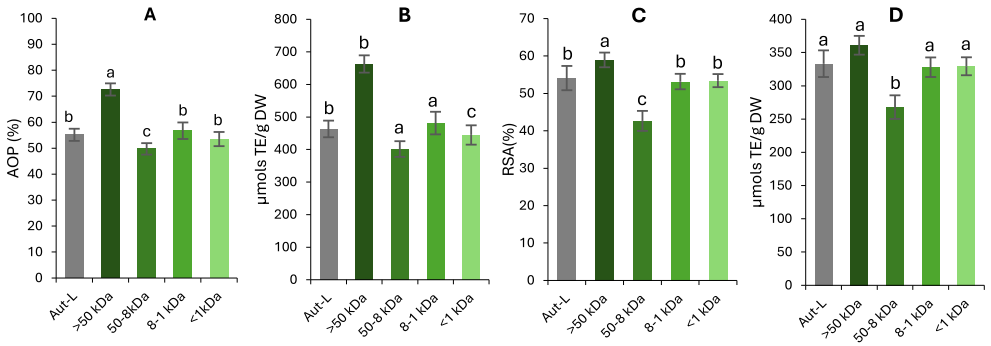

Fig. 3. Antioxidant capacity of Aut-L and the hemicellulose fractions at different molecular weights ranges by means of ABTS (A, B) and DPPH (C, D) assays.

Table 5
Minimum inhibitory concentration (MIC, mg/mL) and minimum bactericidal concentration (MBC, mg/mL) of hemicellulose fractions with different molecular weights against foodborne pathogenic bacteria.

Bacteria	Aut-L		>50 kDa		50–8 kDa		8–1 kDa		1 kDa	
	MBC	MIC	MBC	MIC	MBC	MIC	MBC	MIC	MBC	MIC
L. monocytogenes (3254)	15	13	15	9	nf	12	nf	15	14	9
L. monocytogenes (CETC 4032)	19	9	nf[a]	15	20	18	nf	15	20	15
S. enterica (CETC 704)	19	15	nf	19	nf	nf	nf	20	20	13
E. coli (CETC 4076)	19	15	nf	nf	nf	nf	nf	20	20	13
S. aureus (103)	20	11	nf	nf	nf	nf	nf	20	20	11
S. aureus (33)	20	12	nf	19	nf	nf	nf	16	18	13

[a] nf refers to not found at the tested concentrations.

effectively preserved the transparency of PVA. In contrast, higher Mw-range fractions may potentially induce film opacity through phase separation dynamics [40].

Films containing 10 wt% APW-hemicelluloses exhibiting UV-light blocking values exceeding 80 %. The enhanced UV-blocking capacity of films enriched with low-Mw hemicelluloses (8–1 kDa and <1 kDa) can be attributed to their significant elevated phenolic content [41]. Therefore, incorporating APW-hemicelluloses of varying Mw in polymeric films seems to be a suitable approach to obtain packaging materials with high antioxidant capacity and UV-light barrier properties, which can help extend the shelf life of food while minimizing loss of transparency thus preserving sensory attributes [42]. However, Mw is a critical factor influencing the mechanical performance and physical properties of composite materials. Consequently, the final phase of this study evaluated the mechanical and physical properties of APW-hemicellulose enriched PVA films across different Mw- ranges [43].

3.2.3. *Mechanical performance and physical properties of APW-hemicellulose films*

The mechanical properties, specifically Young's Modulus (YM) and Tensile Strength (TS) are presented in Fig. 4E–F. Generally, films containing high Mw-range fractions (>50 kDa and 50–8 kDa) exhibited higher TS values. Notably, the most significant reinforcement effect was observed in the 15 wt% films containing the 50–8 kDa fraction, showing a 67 % improvement over neat PVA. In contrast, the use of >50 kDa fraction provided a more modest enhancement (25 % over neat PVA). A similar trend was observed for YM with 15 wt% of >50 kDa and 50–8 kDa films exhibiting the highest values. However, it appeared that hemicellulose proportions exceeding 15 wt% led to a decline in the mechanical performance of the films. This reduction is likely due to inadequate dispersion of the polysaccharides within the matrix, resulting in weaker films. Generally, when the optimal proportion is surpassed, negative effects on reinforcement properties arise due to the formation of aggregates [44]. Notably, significant differences were observed among hemicelluloses of varying molecular weight ranges. Higher molecular weight (Mw) hemicelluloses demonstrated a superior reinforcement effect, likely attributable to the formation of a more compact matrix. Additionally, these high Mw hemicelluloses exhibited a higher Xyl/Ara ratio (43.07/3.64, as shown in Table 3), indicating a greater proportion of linear chain structures that enhance mechanical properties [10]. This effect aligns with previous findings on polysaccharide films derived from coffee ground polysaccharide-rich fractions [40]. No discernible differences were found between the 8–1 kDa and <1 kDa fractions, as both displayed similar strain-deformation responses under stress (Fig. S5). As previously mentioned, these MMCO exhibited comparable weight-average molar masses and Mw distributions, resulting in negligible differences in film performance.

Physical properties are displayed in Fig. 4G–H. The results indicated that hemicellulose-enriched PVA films exhibited more hydrophilic behavior under saturated water conditions. Swelling degree (SD) results revealed that APW-hemicellulose films had increased water absorption capacity across all proportions, except for 20 wt%, compared to neat PVA. The incorporation of hemicelluloses enhanced the porous structure of the films, facilitating greater water retention [45]. The hydrophilic nature of the film components also contributed to increased solubility. The influence of MMCO was significantly pronounced, with low Mw-range hemicellulose films demonstrating a high SD (766.67 % for the 5 wt% <1 kDa film) and the lowest solubility value (8.4 %). Hemicelluloses are characterized by a low degree of polymerization and a high number of hydroxyl groups, which enable rapid water absorption in hemicellulose-enriched PVA films [41]. The MMCO effect enhances this absorption by increasing the exposure of hydrophilic groups per DW. Furthermore, films with higher concentrations of APW-hemicelluloses and elevated Mw ranges exhibited decreased resistance to water ingress, as these fractions contributed to increased film porosity, facilitating water movement. This suggests that high Mw-range hemicelluloses (>50 and 50–8 kDa) may enhance water molecule mobility within the films. The agglomeration effect resulting from electrostatic interactions intensified with rising hemicellulose concentration [38]. Conversely, low Mw-range hemicelluloses displayed comparable or lower water vapor permeability (WVP) compared to neat PVA films due to the presence of a tortuous pathway (Fig. S6). Water vapor molecules became trapped within this labyrinthine structure, allowing only a limited number of molecules to escape from the PVA matrix [41].

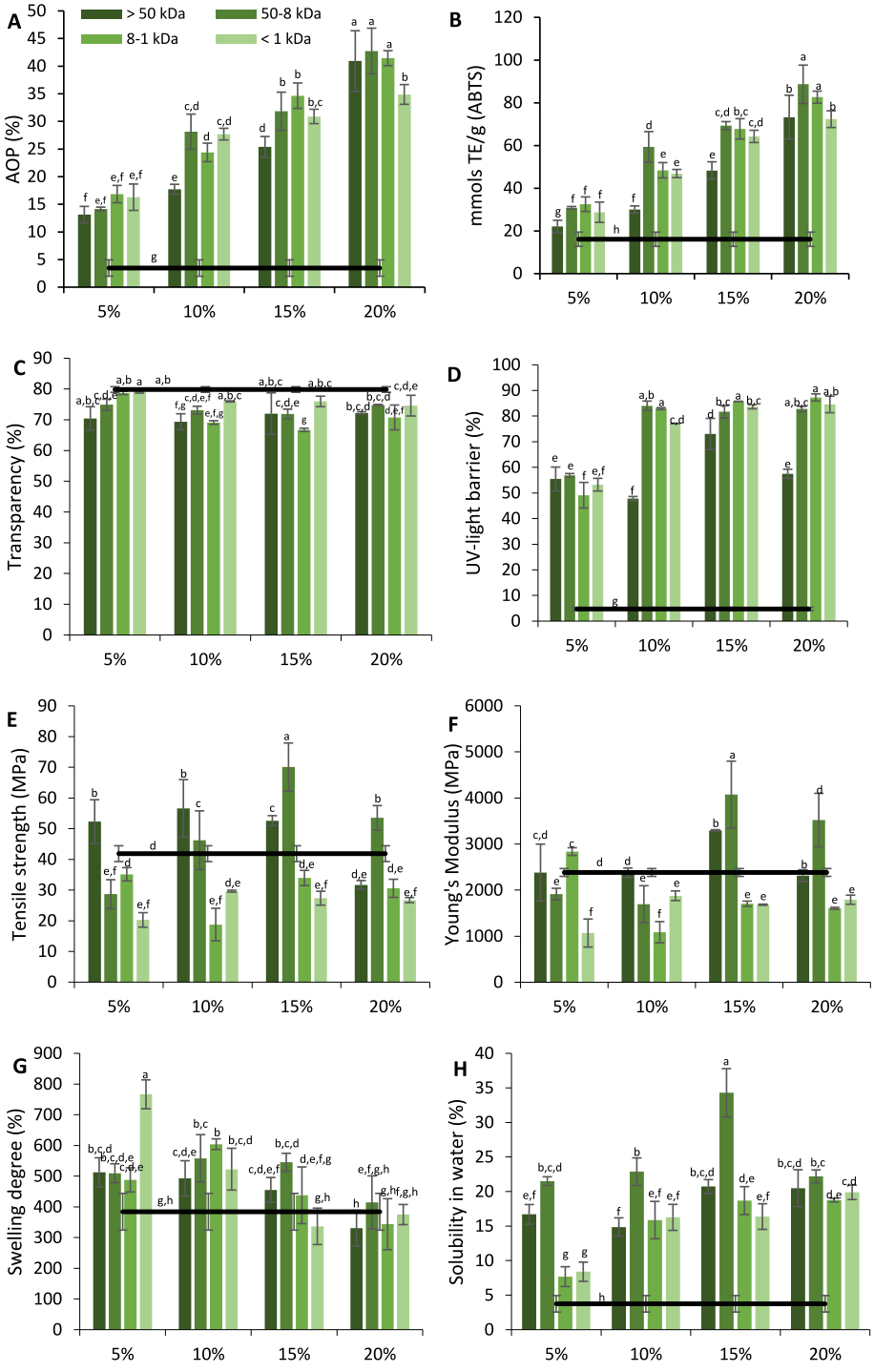

Fig. 4. Antioxidant activity (A,B), optical (C,D), mechanical (E,F) and physical (G,H) properties from PVA-based films enriched with APW-hemicelluloses with different molecular weights at increasing proportions.

3.2.4. *Biodegradability of APW-hemicellulose films*

One of the main challenges associated with food packaging is its persistent environmental impact [46]. For this reason, the development of alternative materials that degrade under natural conditions has become essential. PVA is biodegradable by nature, but it is necessary to corroborate the maintenance of this property by incorporating other compounds in the film formulation such as hemicelluloses. Thus, the biodegradability of the films was evaluated in terms of their weight loss (WL) as indicator after a period of 50 days of burial in soil under controlled conditions [47]. To this end, films with lower and higher hemicellulose content (5 and 20 wt%) were analyzed at all MMCOs studied and the results are shown in Fig. 5.

It was observed that films with higher hemicellulose content (20 wt %) exhibited greater WL compared to those with lower hemicellulose content (5 wt%). This suggests that increased hemicellulose concentration enhances microbial degradation. This effect may be attributed to hydrophilic nature of hemicelluloses, which facilitates enzymatic and microbial degradation [48]. Among the hemicellulose fractions, the films containing 20 wt% of the highest Mw fractions (>50 kDa) exhibited the greatest biodegradation (59.38 ± 3.66 % WL). This trend

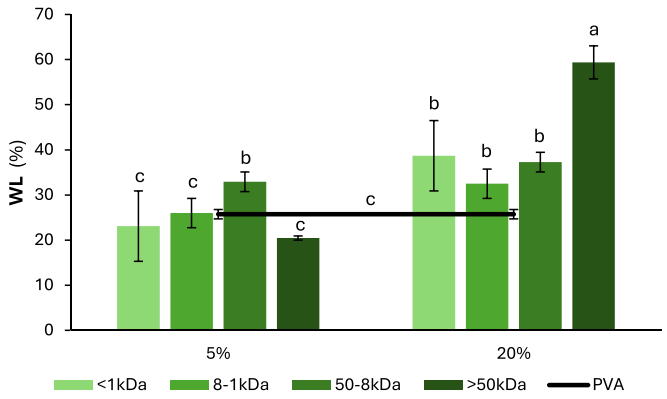

Fig. 5. Weight Loss (WL, %) of PVA-based films enriched with APW-hemicelluloses with different molecular weights at 5 and 20 wt% after 50 days of soil burial.

is in line with the results published in literature, where larger hemicellulose molecules contribute to increased water absorption and microbial accessibility, promoting degradation [49]. These biodegradation values align with previous studies on natural fiber-based biopolymers. Similarly, a bio-based film composed of 50 % xylan and PVA exhibited 56 % WL after 30 days, whereas a 25 % xylan-PVA film reached 42.2 % WL in the same period [50]. However, WL values in the present study are significantly lower than those reported for xylan and gelatin-based films which exhibited over 100 % WL in 15 days. The differences can be attributed to the polymer matrix composition. PVA is known for its biodegradability [51] but when it is blended with some recalcitrant compounds, such as lignin, the biodegradation rate decreases, as lignin restricts enzymatic accessibility to the polymer matrix [52]. These findings suggest that the Mw and compositional characteristics of hemicelluloses influence the interactions with other polymers, playing a crucial role in determining their biodegradation rates.

4. Conclusions

The valorization of APW has been carried out by sustainable obtention of different Mw range hemicelluloses with a high process yield (71.85 %). The hemicelluloses presented a suitable carbohydrate and phenolic acid profile, as well as high antioxidant and antimicrobial capacity suggesting their suitability as active ingredients in packaging formulations. A structural study was carried out to find out how the presence of hemicelluloses of various Mw ranges affected the PVA films. It was found that, in addition to providing bioactive properties, the high Mw fractions exerted a reinforcing effect, achieving 67 % improvements in terms of tensile strength. Finally, the evaluation of the physical properties of the hemicellulose-enriched PVA films revealed high barrier capacity against water vapor, especially those that included low Mw-range hemicelluloses. On the other hand, it was demonstrated that the PVA films enriched with APW-hemicelluloses had a high solubility in water, which could contribute to biodegradability. The biodegradability high Mw hemicellulose enriched PVA-films exhibited higher degradation rate reaching 59 % weight loss. Moreover, the food-grade status of the hemicelluloses needs to be confirmed in further investigation to ensure safety for direct food contact and suitability for sustainable active food packaging.

CRediT authorship contribution statement

Andrea Lucena: Writing – original draft, Methodology, Investigation, Formal analysis, Data curation, Conceptualization. **Esther Rincón:** Writing – review & editing, Writing – original draft, Supervision, Methodology, Investigation, Formal analysis, Data curation, Conceptualization. **Pamela Freire de Moura Pereira:** Writing – original draft, Investigation, Formal analysis, Data curation. **Amparo Jiménez-Quero:** Writing – review & editing, Supervision, Methodology. **Alejandro Rodríguez:** Writing – review & editing, Validation, Project administration, Funding acquisition. **Fernando Pérez-Rodríguez:** Validation, Project administration, Methodology, Funding acquisition, Formal analysis. **Eduardo Espinosa:** Writing – review & editing, Validation, Supervision, Project administration, Investigation, Conceptualization.

Declaration of competing interest

The authors declare that they have no known competing financial interests or personal relationships that could have appeared to influence the work reported in this paper.

Acknowledgments

The authors acknowledge gratitude for the financial support provided by the Ministerio de Ciencia e Innovación (MCINN) of Spain through national project PID2020-117718RB-I00, as part of the national programme of R + D projects "Retos Investigación" y "Generación de Conocimiento," funded by MCIN/AEI/10.13039/501100011033. This work was supported by European Union's Horizon 2020 Research and Innovation programme (A.J-Q and P.F.M.P, project SISTERS, Grant Agreement number 101037796).

Appendix A. Supplementary data

Supplementary data to this article can be found online at https://doi.org/10.1016/j.ijbiomac.2025.142982.

Data availability

Data will be made available on request.

References

[1] E. Espinosa, E. Rincón, L.M. Reyes Mendez, R. Morcillo-Martín, L. Rabasco-Vílchez, J. Moreno-García, J. de Haro, A. Lucena, A. Rodríguez, Lignocellulosic resources: a key player in the transition to a circular bioeconomy, in: A. García-Peñas, G. Sharma (Eds.), New Materials for a Circular Economy, Materials Research Forum, 2023, pp. 393–445, https://doi.org/10.21741/9781644902639-11.
[2] C. Castro-López, I. Bautista-Hernández, M.D. González-Hernández, G.C. G. Martínez-Ávila, R. Rojas, A. Gutiérrez-Díez, N. Medina-Herrera, V.E. Aguirre-Arzola, Polyphenolic profile and antioxidant activity of leaf purified Hydroalcoholic extracts from seven Mexican Persea americana cultivars, Molecules 24 (2019) 173–191, https://doi.org/10.3390/molecules24010173.
[3] J. Soria-González, R. Tauro, J. Alvarado-Flores, V. Berrueta-Soriano, J. Rutiaga-Quiñones, Avocado tree pruning pellets (Persea americana mill.) for energy purposes: characterization and quality evaluation, Energies (Basel) 15 (2022) 7514–7532, https://doi.org/10.3390/en15207514.
[4] P. Jimenez, P. Garcia, V. Quitral, K. Vasquez, C. Parra-Ruiz, M. Reyes-Farias, D. F. Garcia-Diaz, P. Robert, C. Encina, J. Soto-Covasich, Pulp, leaf, Peel and seed of avocado fruit: a review of bioactive compounds and healthy benefits, Food Rev. Int. 37 (2020) 619–655, https://doi.org/10.1080/87559129.2020.1717520.
[5] Y. Zhao, H. Sun, B. Yang, Y. Weng, Hemicellulose-based film: potential green films for food packaging, Polymers-Basel. 12 (2020) 1775–1789, https://doi.org/10.3390/polym12081775.
[6] F. Khalili, H. Amiri, Integrated processes for production of cellulosic and hemicellulosic biobutanol from sweet sorghum bagasse using autohydrolysis, Ind. Crop Prod. 145 (2020) 111918, https://doi.org/10.1016/j.indcrop.2019.111918.
[7] M. Ramos-Andrés, B. Aguilera-Torre, J. García-Serna, Production of purified hemicellulose-pectin fractions of different molecular weight from discarded carrots by hydrothermal treatment followed by multistep ultrafiltration/diafiltration, J. Clean. Prod. 321 (2021) 128923, https://doi.org/10.1016/j.jclepro.2021.128923.
[8] P. Nechita, R. Mirela, F. Ciolacu, Xylan hemicellulose: a renewable material with potential properties for food packaging applications, Sustainability 13 (2021) 13504–13520, https://doi.org/10.3390/su132413504.
[9] J. Rao, Z. Lv, G. Chen, F. Peng, Hemicellulose: structure, chemical modification, and application, Prog. Polym. Sci. 140 (2023) 101675, https://doi.org/10.1016/j.progpolymsci.2023.101675.
[10] X. Jin, Z. Hu, S. Wu, T. Song, F. Yue, Z. Xiang, Promoting the material properties of xylan-type hemicelluloses from the extraction step, Carbohydr. Polym. 215 (2019) 235–245, https://doi.org/10.1016/j.carbpol.2019.03.092.

[11] Technical Association of the Pulp and Paper Industry (TAPPI), Technical Association of the Pulp and Paper Industry (TAPPI) standards: regulation and style guidelines. http://www.tappi.org/content/pdf/standards/tm_guidelines_complete.pdf, 2018. (Accessed 4 September 2024).
[12] E. Espinosa, E. Rincón, R. Morcillo-Martín, L. Rabasco-Vílchez, A. Rodríguez, Orange peel waste biorefinery in multi-component cascade approach: polyphenolic compounds and nanocellulose for food packaging, Ind. Crop Prod. 187 (2022) 115413, https://doi.org/10.1016/j.indcrop.2022.115413.
[13] O.M. Bonilla-Luque, A. Possas, M.L. Cabo, P. Rodríguez-López, A. Valero, Tracking microbial quality, safety and environmental contamination sources in artisanal goat cheesemaking factories, Food Microbiol. 114 (2023) 104301, https://doi.org/10.1016/j.fm.2023.104301.
[14] M. Sánchez-Gutiérrez, I. Bascón-Villegas, A. Rodríguez, F. Pérez-Rodríguez, Á. Fernández-Prior, A. Rosal, E. Carrasco, Valorisation of Olea europaea L, Olive Leaves through the Evaluation of Their Extracts: Antioxidant and Antimicrobial Activity, Foods 10 (2021) 966–985, https://doi.org/10.3390/foods10050966.
[15] E. Rincón, E. Espinosa, M.T. García-Domínguez, A.M. Balu, F. Vilaplana, L. Serrano, A. Jiménez-Quero, Bioactive pectic polysaccharides from bay tree pruning waste: sequential subcritical water extraction and application in active food packaging, Carbohydr. Polym. 272 (2021) 118477, https://doi.org/10.1016/j.carbpol.2021.118477.
[16] A. International, ASTM D882–18, Standard Test Method for Tensile Propertes of Thin Plastic Sheetings, 2018.
[17] E. Rincón, J. De Haro-Niza, R. Morcillo-Martín, E. Espinosa, A. Rodríguez, Boosting functional properties of active-CMC films reinforced with agricultural residues-derived cellulose nanofibres, RSC Adv. 13 (2023) 24755–24766, https://doi.org/10.1039/D3RA04003H.
[18] A. International, ASTM E96 / E96M-10, Standard Test Methods for Water Vapor Transmission of Materials, 2010.
[19] R. Morcillo-Martín, L. Rabasco-Vílchez, F. Jiménez-Jiménez, E. Espinosa, Q. Tarrés, A. Rodríguez, Thermoformed Fiber-polyethylene biocomposites: a circular food packaging on cherry tomatoes, Food Bioproc. Tech. (2024), https://doi.org/10.1007/s11947-024-03610-x.
[20] P.R.S. Páramos, J.F.O. Granjo, M.L. Corazza, H.A. Matos, Extraction of high value products from avocado waste biomass, J. Supercrit. Fluid. 165 (2020) 104988, https://doi.org/10.1016/j.supflu.2020.104988.
[21] S.V. Obydenkova, P.D. Kouris, D.M.J. Smeulders, M.D. Boot, Y. van der Meer, Evaluation of environmental and economic hotspots and value creation in multi-product lignocellulosic biorefinery, Biomass Bioenergy 159 (2022) 106394, https://doi.org/10.1016/j.biombioe.2022.106394.
[22] I. Dávila, B. Gullón, J. Labidi, P. Gullón, Multiproduct biorefinery from vine shoots: bio-ethanol and lignin production, Renew. Energy 142 (2019) 612–623, https://doi.org/10.1016/j.renene.2019.04.131.
[23] E. Rincón, A. Zuliani, A. Jiménez-Quero, F. Vilaplana, R. Luque, L. Serrano, A. M. Balu, Combined extraction/purification-catalytic microwave-assisted conversion of Laurus nobilis L. pruning waste polysaccharides into methyl levulinate, ACS Sustain. Chem. Eng. 8 (2020) 11016–11023, https://doi.org/10.1021/acssuschemeng.0c04161.
[24] M. Ramos-Andrés, C. Andrés-Iglesias, J. García-Serna, Production of molecular weight fractionated hemicelluloses hydrolyzates from spent coffee grounds combining hydrothermal extraction and a multistep ultrafiltration/diafiltration, Bioresour. Technol. 292 (2019) 121940, https://doi.org/10.1016/j.biortech.2019.121940.
[25] B.M. Harahap, Degradation techniques of hemicellulose fraction from biomass feedstock for optimum xylose production: a review, Jurnal Keteknikan Pertanian Tropis Dan Biosistem 8 (2020) 107–124, https://doi.org/10.21776/ub.jkptb.2020.008.02.01.
[26] A. Siemińska-Kuczer, M. Szymańska-Chargot, A. Zdunek, Recent advances in interactions between polyphenols and plant cell wall polysaccharides as studied using an adsorption technique, Food Chem. 373 (2022) 31487, https://doi.org/10.1016/j.foodchem.2021.131487.
[27] E. Ankona, V. Multanen, M. Nisnevitch, M. Billig, Y. Anker, Investigation of pyrolysis kinetics and gaseous compounds emitted during charcoal production from woods commonly used in the eastern Mediterranean, Biofuels Bioprod. Biorefin. 15 (2021) 646–656, https://doi.org/10.1002/bbb.2188.
[28] O.M. Terrett, J.J. Lyczakowski, L. Yu, D. Iuga, W.T. Franks, S.P. Brown, R. Dupree, P. Dupree, Molecular architecture of softwood revealed by solid-state NMR, Nat. Commun. 10 (2019) 4978, https://doi.org/10.1038/s41467-019-12979-9.
[29] F. Campos, A.F. Peixoto, P.A.R. Fernandes, M.A. Coimbra, N. Mateus, V. de Freitas, I. Fernandes, A. Fernandes, The antidiabetic effect of grape pomace polysaccharide-polyphenol complexes, Nutrients 13 (2021) 4495–4513, https://doi.org/10.3390/nu13124495.
[30] R. Requena, A. Jiménez-Quero, M. Vargas, R. Moriana, A. Chiralt, F. Vilaplana, Integral fractionation of Rice husks into bioactive Arabinoxylans, cellulose nanocrystals, and silica particles, ACS Sustain. Chem. Eng. 7 (2019) 6275–6286, https://doi.org/10.1021/acssuschemeng.8b06692.
[31] P. Rozi, A. Abuduwaili, P. Mutailifu, Y. Gao, R. Rakhmanberdieva, H.A. Aisa, A. Yili, Sequential extraction, characterization and antioxidant activity of polysaccharides from Fritillaria pallidiflora Schrenk, Int. J. Biol. Macromol. 131 (2019) 97–106, https://doi.org/10.1016/j.ijbiomac.2019.03.029.
[32] H. Guo, M.-X. Fu, D.-T. Wu, Y.-X. Zhao, H. Li, H.-B. Li, R.-Y. Gan, Structural characteristics of crude polysaccharides from 12 selected Chinese teas, and their antioxidant and anti-diabetic activities, Antioxidants 10 (2021) 1562–1576, https://doi.org/10.3390/antiox10101562.
[33] M. Jesus, A. Romaní, F. Mata, L. Domingues, Current options in the valorisation of vine pruning residue for the production of biofuels, Biopolymers, Antioxidants, and Bio-Composites following the Concept of Biorefinery: A Review, Polymers-Basel 14 (2022) 1640–1661, https://doi.org/10.3390/polym14091640.
[34] X. Liu, X. Li, Y. Bai, X. Zhou, L. Chen, C. Qiu, C. Lu, Z. Jin, J. Long, Z. Xie, Natural antimicrobial oligosaccharides in the food industry, Int. J. Food Microbiol. 386 (2023) 110021, https://doi.org/10.1016/j.ijfoodmicro.2022.110021.
[35] Z. Wang, Q. Sun, H. Zhang, J. Wang, Q. Fu, H. Qiao, Q. Wang, Insight into antibacterial mechanism of polysaccharides: a review, LWT–Food Sci. Technol. 150 (2021) 111929, https://doi.org/10.1016/j.lwt.2021.111929.
[36] F. Khan, N.I. Bamunuarachchi, N. Tabassum, Y.-M. Kim, Caffeic acid and its derivatives: antimicrobial drugs toward microbial pathogens, J. Agric. Food Chem. 69 (2021) 2979–3004, https://doi.org/10.1021/acs.jafc.0c07579.
[37] A. Pandi, V.M. Kalappan, Pharmacological and therapeutic applications of Sinapic acid—an updated review, Mol. Biol. Rep. 48 (2021) 3733–3745, https://doi.org/10.1007/s11033-021-06367-0.
[38] S. Rivas, E. Conde, A. Moure, H. Domínguez, J.C. Parajó, Characterization, refining and antioxidant activity of saccharides derived from hemicelluloses of wood and rice husks, Food Chem. 141 (2013) 495–502, https://doi.org/10.1016/j.foodchem.2013.03.008.
[39] W. Yang, H. Ding, G. Qi, C. Li, P. Xu, T. Zheng, X. Zhu, J.M. Kenny, D. Puglia, P. Ma, Highly transparent PVA/nanolignin composite films with excellent UV shielding, antibacterial and antioxidant performance, React. Funct. Polym. 162 (2021) 104873, https://doi.org/10.1016/j.reactfunctpolym.2021.104873.
[40] M. Alee, Q. Duan, Y. Chen, H. Liu, A. Ali, J. Zhu, T. Jiang, A. Rahaman, L. Chen, L. Yu, Plasticization efficiency and characteristics of monosaccharides, disaccharides, and low-molecular-weight polysaccharides for starch-based materials, ACS Sustain. Chem. Eng. 9 (2021) 11960–11969, https://doi.org/10.1021/acssuschemeng.1c04374.
[41] E. Espinosa, I. Bascón-Villegas, A. Rosal, F. Pérez-Rodríguez, G. Chinga-Carrasco, A. Rodríguez, PVA/(ligno)nanocellulose biocomposite films. Effect of residual lignin content on structural, mechanical, barrier and antioxidant properties, Int. J. Biol. Macromol. 141 (2019) 197–206, https://doi.org/10.1016/j.ijbiomac.2019.08.262.
[42] P. Ezati, A. Khan, R. Priyadarshi, T. Bhattacharya, S.K. Tammina, J.-W. Rhim, Biopolymer-based UV protection functional films for food packaging, Food Hydrocoll. 142 (2023) 108771, https://doi.org/10.1016/j.foodhyd.2023.108771.
[43] D. Domene-López, J.C. García-Quesada, I. Martin-Gullon, M.G. Montalbán, Influence of starch composition and molecular weight on physicochemical properties of biodegradable films, Polymers-Basel 11 (2019) 1084–1101, https://doi.org/10.3390/polym11071084.
[44] D. Sutay Kocabaş, M. Erkoç Akçelik, E. Bahçegül, H.N. Özbek, Bulgur bran as a biopolymer source: production and characterization of nanocellulose-reinforced hemicellulose-based biodegradable films with decreased water solubility, Ind. Crop. Prod. 171 (2021) 113847, https://doi.org/10.1016/j.indcrop.2021.113847.
[45] T. Lei, R. Zhang, Y. Liu, X. Zhu, K. Li, G. Li, H. Zheng, Effect of the high barrier and hydrophobic hemicellulose/montmorillonite film on postharvest quality of fresh green asparagus, Ind. Crop. Prod. 187 (2022) 115509, https://doi.org/10.1016/j.indcrop.2022.115509.
[46] V. Guillard, S. Gaucel, C. Fornaciari, H. Angellier-Coussy, P. Buche, N. Gontard, The next generation of sustainable food packaging to preserve our environment in a circular economy context, Front. Nutr. 5 (2018), https://doi.org/10.3389/fnut.2018.00121.
[47] F. Bueno, L. Fultz, C. Husseneder, M. Keenan, S. Sathivel, Biodegradability of bacterial cellulose polymer below the soil and its effects on soil bacteria diversity, Polym. Degrad. Stab. 217 (2023) 110535, https://doi.org/10.1016/j.polymdegradstab. 2023.110535.
[48] I. Surya, C.M. Hazwan, H.P.S. Abdul Khalil, E.B. Yahya, A.B. Suriani, M. Danish, A. Mohamed, Hydrophobicity and biodegradability of Silane-treated Nanocellulose in biopolymer for high-grade packaging applications, Polymers (Basel) 14 (2022) 4147, https://doi.org/10.3390/polym14194147.
[49] M.M. Abe, M.C. Branciforti, M. Brienzo, Biodegradation of hemicellulose-cellulose-starch-based bioplastics and microbial polyesters, Recycling 6 (2021) 22, https://doi.org/10.3390/recycling6010022.
[50] S. Wang, J. Ren, W. Li, R. Sun, S. Liu, Properties of polyvinyl alcohol/xylan composite films with citric acid, Carbohydr. Polym. 103 (2014) 94–99, https://doi.org/10.1016/j.carbpol.2013.12.030.
[51] B. Tan, Y. Ching, S. Poh, L. Abdullah, S. Gan, A review of natural fiber reinforced poly(vinyl alcohol) based composites: application and opportunity, Polymers (Basel) 7 (2015) 2205–2222, https://doi.org/10.3390/polym7111509.
[52] C. Deng, X. Kang, R. Lin, B. Wu, X. Ning, D. Wall, J.D. Murphy, Boosting biogas production from recalcitrant lignin-based feedstock by adding lignin-derived carbonaceous materials within the anaerobic digestion process, Energy 278 (2023) 127819, https://doi.org/10.1016/j.energy.2023.127819.